Fusome morphogenesis is sufficient to promote female germline stem cell self-renewal in *Drosophila*

Amanda M. Powell[1], Anna E. Williams[1,2], and Elizabeth T. Ables[1]*

[1]Department of Biology, East Carolina University, Greenville, NC, 27858

[2]Current address: Biochemistry, Cell and Developmental Biology Graduate Program, Emory University, Atlanta, GA, 30322

*Correspondence: ablese@ecu.edu; 1001 E. 10th St. Mailstop 552, Greenville, NC 27858; Phone: 252-328-9770

RUNNING TITLE

Tnpo-SR promotes fusome morphogenesis

KEYWORDS

Oogenesis, Tnpo-SR, ovary, beta-importin

CORRESPONDING AUTHOR:

Elizabeth T. Ables

East Carolina University

Department of Biology

1001 E. 10th St., Mailstop 551

553 Science & Technology Building

Greenville, NC 27858

Office phone: 252-328-9770

e-mail: ablese@ecu.edu

Abstract

Many tissue-resident stem cells are retained through asymmetric cell division, a process that ensures stem cell self-renewal through each mitotic cell cycle. Asymmetric organelle distribution has been proposed as a mechanism by which stem cells are marked for long-term retention; however, it is not clear whether biased organelle localization is a cause or an effect of asymmetric division. In *Drosophila* females, an endoplasmic reticulum-like organelle called the fusome is continually regenerated in germline stem cells (GSCs) and associated with GSC division. Here, we report that the β-importin Tnpo-SR is essential for fusome regeneration. Depletion of *Tnpo-SR* disrupts cytoskeletal organization during interphase and nuclear membrane remodeling during mitosis. Tnpo-SR does not localize to microtubules, centrosomes, or the fusome, suggesting that its role in maintaining these processes is indirect. Despite this, we find that restoring fusome morphogenesis in *Tnpo-SR*-depleted GSCs is sufficient to rescue GSC maintenance and cell cycle progression. We conclude that Tnpo-SR functionally fusome regeneration to cell cycle progression, supporting the model that asymmetric rebuilding of fusome promotes maintenance of GSC identity and niche retention.

Summary Statement

Regeneration of the fusome, an ER-like organelle in *Drosophila* female germline stem cells, relies on Tnpo-SR-dependent reorganization of the microtubule network during interphase.

Introduction

Stem cells maintain cellular diversity in tissues undergoing regeneration, repair, or remodeling (Das et al., 2020; de Morree and Rando, 2023). The long-term maintenance of stem cells within tissues requires molecular mechanisms that effectively balance stem cell self-renewal with differentiation to a committed cell fate (Knoblich, 2008; Li and Xie, 2005). Among these, asymmetric cell division (ACD) is a conserved process in which two cells of unequal fates are produced at each round of mitosis (Chen and Yamashita, 2021; Sunchu and Cabernard, 2020). This allows a self-renewing population of stem cells to be retained in tissues even as differentiated daughters are continually produced. ACD can be achieved by differential reception of extrinsic factors or by asymmetric localization of intrinsic cell fate determinants like proteins, mRNA, or organelles. Although many stem cells display unequal partitioning of organelles at mitosis, the extent to which organelle localization promotes self-renewal remains unclear.

Drosophila female germline stem cells (GSCs) are an excellent genetic and cell biological model of ACD (Hinnant et al., 2020; Venkei and Yamashita, 2015). GSCs reside at the anterior end of ovarioles (the oocyte-producing units of the ovary) and are established during development in a somatic niche composed of cap cells and terminal filament cells (Figure 1A). GSCs divide perpendicular to the niche, such that each mitotic division creates one daughter cell destined for differentiation (called the cystoblast) and one stem cell, which remains anchored to the cap cells via adherens junctions. The GSC and the cystoblast remain connected through an intracellular bridge following mitosis through G_2 phase of the next cell cycle, when the ring canal constricts and abscission occurs (Figure 1B) (Ables and Drummond-Barbosa, 2013; Villa-Fombuena et al., 2021). The cystoblast goes on to divide exactly four times with incomplete cytokinesis forming 16-cell cysts, from which, one oocyte will be specified. Thus, each mitotic division of the GSC has the potential to create one differentiated oocyte.

Previous studies demonstrate that at least three distinct organelles (nucleolar/ribosome complexes, centrosomes, and fusomes) are asymmetrically distributed in GSCs (de Cuevas and Spradling, 1998; Fichelson et al., 2009; Yamashita

et al., 2007). Among these, the fusome is arguably the most well-characterized, in large part due to a preponderance of available molecular markers for its visualization (Hinnant et al., 2020; Lighthouse et al., 2008; Williams and Ables, 2023). The fusome (also called the spectrosome in GSCs) is a cytoplasmic structure composed of endoplasmic reticulum-like membranous vesicles and a spectrin/spectraplankin cytoskeletal core that elongates during the cell cycle and is partitioned to the cystoblast (Figure 1B) (de Cuevas et al., 1996; de Cuevas et al., 1997; Lighthouse et al., 2008; Snapp et al., 2004). Fusome material accumulates at each mitotic division, concomitant with the disassembly of the mitotic spindle (de Cuevas and Spradling, 1998; Diegmiller et al., 2023; Koch and King, 1966; Lin et al., 1994; Mahowald, 1971). For much of their cell cycle, GSCs have a large, round fusome anchored at the anterior margin of the cell, closest to the neighboring somatic cap cells (de Cuevas and Spradling, 1998; Huynh, 2006; Ong et al., 2010; Villa-Fombuena et al., 2021). During GSC mitosis, a small plug of fusome material is deposited at the central spindle, foreshadowing placement of the intracellular bridge that forms between the GSC and the presumptive cystoblast. The fusome likely aids in the establishment and maintenance of this intracellular bridge, similar to other systems (Chaigne and Brunet, 2022; Li et al., 2024; Ong et al., 2010; Spradling, 2024). As the GSC transitions from G_1 to S, the nascent fusome in the ring canal builds anteriorly to join with the fusome material that remained at the cap cell interface. The fusome is eventually severed between the GSC and the cystoblast when abscission occurs in G_2 (resulting in an “exclamation point” morphology; Figure 1B). Following abscission, the GSC fusome retracts and condenses to a round morphology. The fusome is therefore asymmetrically inherited at mitosis, as the GSC always retains more organelle material than the cystoblast (de Cuevas and Spradling, 1998; Huynh, 2006).

Despite the well-characterized morphogenesis of the fusome, it is not clear whether the fusome *per se* is essential for GSC self-renewal. In germ cells lacking core cytoskeletal fusome components like β-spectrin or the adducin homolog *hu li tai shao* (*hts*), fusomes fail to form (as visualized by α-Tubulin and α-Spectrin localization) and germ cells largely fail to form cysts. However, it is unclear whether GSCs are retained in the niche, since Hts and α-Spectrin are also key tools for GSC identification (de Cuevas

et al., 1996; Röper, 2007). Similarly, loss of the recycling endosome protein Rab11, which is enriched in the GSC fusome, is essential for both fusome morphogenesis and maintenance of GSCs (Bogard et al., 2007; Lighthouse et al., 2008). In contrast, loss of the fusome-enriched proteins Scribble or Tropomodulin do not impact fusome structure (as visualized by Hts localization) or GSC maintenance (Lighthouse et al., 2008). Thus, while not every fusome-enriched protein is necessary for GSC self-renewal, the question of whether the fusome promotes GSC identity remains unresolved.

Here, we take advantage of a genetic model in which GSC fusome morphogenesis is impaired to explore the connection between GSC maintenance and fusome/ER asymmetric inheritance. We previously demonstrated that the β-importin encoded by *Transportin-Serine/Arginine rich* (*Tnpo-SR*) is necessary for GSC self-renewal, development of 16-cell cysts, and timely oocyte specification (Beachum et al., 2023). Extending these observations, we find that although Tnpo-SR does not localize to the fusome, it is essential to rebuild the fusome at each cell cycle, impacting the cytoskeletal core, ER-like membranes, and fusome-associated proteins. Consistent with the roles of other β-importins, our data suggests that *Tnpo-SR* promotes nuclear envelope remodeling at mitosis and suppresses microtubule growth from centrosomes during interphase. We also identify the microtubule binding protein encoded by *abnormal spindle* (*asp*) as a putative Tnpo-SR binding partner. Intriguingly, however, over-expression of Asp in *Tnpo-SR*-depleted GSCs does not rescue GSC self-renewal. Instead, we find that over-expression of the fusome component, Hts, the polarity protein Bazooka (Baz)/Par-3, or a Kinesin heavy chain fusion protein (Khc::nod::lacZ) are sufficient to restore fusome area and re-establish GSC self-renewal in *Tnpo-SR*-depleted GSCs. Taken together, these results suggest that rebuilding the microtubule-based fusome core at successive cell cycles builds an intracellular trafficking system that is essential to maintain the GSC fate.

Results

Tnpo-SR promotes regeneration of the GSC fusome during successive cell cycles.

Our previous work revealed that loss of *Tnpo-SR* reduced accumulation of Hts at the fusome at all phases of the cell cycle (Beachum et al., 2023). Indeed, further analysis demonstrated that depletion of *Tnpo-SR* in GSCs reduced overall fusome core area, as measured by fluorescence of α-Spectrin (Figure 1C-D, G-H) or Hts (Figure 1E-F, G-H). The reduction of core area in *Tnpo-SR*-depleted GSCs also impacted accumulation of fusome-associated proteins, such as the apicobasal scaffolding protein Scribble (Scrib; Figure 1C'-D', G-H), and the fusomal membrane protein, Reticulon-like1 (Rtnl1; Figure 1E'-F', G-H). Intriguingly, although overall fusome area was reduced, the dynamic movements of the fusome at different stages of the cell cycle were largely normal in the absence of *Tnpo-SR* (Figure 2). Fusome morphologies consistent with all stages of the cell cycle could be readily identified (Figure 2 and 3A), and the overall cycling time (as measured by the percentage of GSCs labeled with the nucleoside analog EdU during a one-hour pulse; Figure 3B) was not drastically altered. Measurements were taken on germaria collected six days after eclosion, and GSCs cycle every 15-16 hours (Villa-Fombuena et al., 2021); therefore, we estimate that the fusome size was reduced ~45% over about nine cell cycles. This suggests that *Tnpo-SR* is necessary to regenerate the fusome in GSCs at each mitotic division.

Tnpo-SR is dispensable for the assembly, maintenance, and function of the mitotic spindle.

Fusome regeneration in GSCs begins during mitosis, as new fusome material is formed from the microtubule remnants of the mitotic spindle (Figure 1B) (Lin et al., 1994; Villa-Fombuena et al., 2021). β-importins have a variety of roles during mitosis, including regulation of mitotic spindle assembly, abscission, and nuclear membrane and nuclear pore assembly, at least in part via sequestration of spindle assembly factors (Askjaer et al., 2002; Beaudet et al., 2017; Beaudet et al., 2020; Chen et al., 2015; Nachury et al., 2001; Wiese et al., 2001). Given the roles of β-importins in mitosis, we

hypothesized that interphase fusome morphogenesis might be impaired in *Tnpo-SR*-depleted GSCs as a secondary consequence of disrupted mitotic spindle assembly. We labeled GSCs with a fluorophore-conjugated α-Tubulin, the mitosis marker phosphorylated Histone H3 (PHH3), and the centrosome core protein Asterless (Asl), using a light fixation protocol at room temperature to permit stabilization of microtubules and identification of GSCs and surrounding niche cells in control and *Tnpo-SR*^{RNAi} germaria (Figure 4A,C) (Grieder et al., 2000; Williams and Ables, 2023). Although some spindles appeared in a wavy shape, we found no significant difference in mitotic spindle length or width between control GSCs and GSCs lacking *Tnpo-SR* (Figure 4A,C,I-J). Since spindle stability relies on the activity of the spindle matrix (Yao et al., 2018), we further tested whether localization or levels of two key *Drosophila* spindle matrix components, Chromator and Megator, were affected by depletion of *Tnpo-SR*. Congruent with previous studies, we found that Chromator localizes to the chromatin during interphase in wild-type GSCs, while Megator is localized to the inter-heterochromatin space, cytoplasm, and nuclear membrane (Figure S1A,C) (Qi et al., 2004; Rath et al., 2004; Yao et al., 2012; Yao et al., 2018). We did not identify any clear differences in the localization of Chromator or Megator between wild-type and *Tnpo-SR*^{RNAi} GSCs during interphase or at mitosis (Figure S1B,D).

We then asked whether the minor spindle abnormalities in *Tnpo-SR*-depleted GSCs impacted chromosome separation. We analyzed localization of the centromeric protein Centromere Identifier (CID, the centromere-specific histone H34 variant), which is essential for proper assembly and function of centromeres and kinetochores, the primary drivers of spindle assembly (Dattoli et al., 2020; Kochendoerfer et al., 2021). Consistent with the largely stable microtubule spindle, the number of CID foci was equivalent between *Tnpo-SR*-depleted and control GSCs (Figure S2A-C). Taken together, these data suggest that assembly, maintenance, and function of the mitotic spindle are largely unaffected by the loss of *Tnpo-SR*.

Tnpo-SR is required for proper remodeling of the GSC nuclear lamina at mitosis.

In contrast to spindle morphology, loss of *Tnpo-SR* caused significant changes in organization of the nuclear lamina during mitosis. Wild-type GSCs undergo a non-canonical semi-closed nuclear envelope breakdown (NEB), retaining an intact but permeable nuclear membrane (Duan et al., 2021). We visualized the fragmented nuclear membrane during mitosis in wild-type GSCs using antibodies raised against LaminB (Figure 4B). In GSCs lacking *Tnpo-SR*, high levels of LaminB localized around DNA during metaphase (Figure 4D,K). This suggests that in the absence of *Tnpo-SR*, the nuclear lamina collapses to surround the DNA, instead of fragmenting around the spindle. Abnormalities in nuclear lamina fragmentation did not appear to disturb centrosome duplication, maturation, or localization. In both controls and *Tnpo-SR*-depleted GSCs, centrosomes [visualized with antibodies against Asl or Pericentrin-like Protein (Plp)] were randomly localized until late-G_2, at which time one centrosome became anchored at the niche adjacent to the round-shaped fusome in preparation for mitosis (Figure S2D-H). We did not detect overt differences in Asl or Plp accumulation. Thus, while we observed that loss of *Tnpo-SR* impacts nuclear lamina fragmentation, the biological significance of this phenotype remains unclear.

Loss of *Tnpo-SR* causes aberrant interphase centrosomal microtubules.

Since our data did not support roles for *Tnpo-SR* in assembly or function of the mitotic spindle, we asked whether improper disassembly of the spindle and regeneration of the fusome in the GSCs caused the reduction in fusome size. Following mitosis, the GSC/cystoblast pair remains connected via a temporary intracellular bridge (Ables and Drummond-Barbosa, 2013; Mathieu et al., 2013). During this time, fusome proteins (including Hts and the kinase Par-1) accumulate in the cytokinetic furrow (Figure 2B-B'), and condense anteriorly in the GSC towards the cap cells (Figure 2C-E') (Villa-Fombuena et al., 2021). As the central spindle disassembles, α-Tubulin becomes tightly associated with Hts, extending the fusome and likely serving as a framework for continued vesicular trafficking (Figure 2D). Following abscission, fusome material (both Hts and α-Tubulin) aggregates at the anterior side of the GSC, retracting away from the cystoblast and re-forming a round structure by mid-G_2 (Figure 2F-G).

GSCs lacking *Tnpo-SR* still disassembled the bulk of microtubules during telophase and correctly formed the central spindle (Figure 2H-I); however, we saw abnormalities in α-Tubulin localization beginning as early as G_1 (Figure 2I-N). Microtubules appeared disorganized, oriented in random directions rather than coalesced towards the fusome or the anterior of the cell (Figure 2I', M', N'). Although α-Tubulin co-localized with Hts at the fusome, the levels of Hts were drastically reduced, particularly during S/G_2 when the fusome typically builds anteriorly. By late G_2, when control cells had already condensed α-Tubulin into a spherical fusome, *Tnpo-SR*-depleted GSCs failed to condense α-Tubulin, and instead appeared to be building microtubules in random directions (Figure 2N-N').

These observations suggested that *Tnpo-SR* might suppress inappropriate microtubule growth during interphase. To test this hypothesis, we again co-localized α-Tubulin with Asl and imaged cells in interphase (Figure 4E-H). In control interphase GSCs, microtubules were observed either at the fusome or the cell cortex (Figure 4E-F). In contrast, microtubules in *Tnpo-SR*-depleted GSCs grew from centrosomes scattered throughout the cell, oriented intracellularly towards the somatic cap cells and occasionally extending to wrap around the cap cells (Figure 4G-H', L). These results confirm that Tnpo-SR normally suppresses microtubule growth and suggest that loss of microtubule organization underlies the failure to regenerate the fusome properly in *Tnpo-SR*-depleted GSCs.

We then asked whether the microtubule defects caused by *Tnpo-SR* depletion impacted progression through the cell cycle, using two independent assays to measure cell cycle phase length. First, since overall fusome structure remained largely intact in *Tnpo-SR*-depleted GSCs (Figure 2), we used the morphology of the fusome as an indicator of cell cycle phase (Figure 1B, 3A) (Villa-Fombuena et al., 2021). Second, we employed the Fly-Fluorescent Ubiquitination-based Cell Cycle Indicator (FUCCI) system to distinguish cell cycle phases using fluorochrome-tagged transgenes that are degraded in parallel with the cell cycle regulators Cyclin B and E2F1 (Figure 3C) (Hinnant et al., 2017; Villa-Fombuena et al., 2021; Zielke et al., 2014). In both assays, and consistent with prior studies, control GSCs were most frequently found in G_2, with a

much smaller population in G_1 and M, which occur in exceedingly short windows of time (Hinnant et al., 2017; Villa-Fombuena et al., 2021). In contrast, *Tnpo-SR*-depleted cells were more likely to be found in G_1, suggesting that G_1 length is at least two times longer than normal (Figure 3A,C). Notably, in both *Tnpo-SR*-depleted and control GSCs, we observed accumulation and co-localization of the mitotic marker PHH3 with DNA during prophase and metaphase, and waning expression during telophase as chromatids separated to opposing poles (Figure 4A,C), suggesting that the length of mitosis is largely unaffected by loss of *Tnpo-SR*. Further, these results are not consistent with centrosome maturation defects, which typically arrest cells in G_2 (Venkei and Yamashita, 2015). We conclude that *Tnpo-SR*-depleted cells delay exit from G_1, perhaps as a consequence of inappropriate microtubule regulation or improper NEB.

Tnpo-SR does not localize to centrosomes or the fusome.

Given that loss of *Tnpo-SR* caused defects in fusome regeneration and centrosome-dependent microtubule dynamics, we hypothesized that it might function in GSCs by directly binding proteins associated with these organelles, facilitating intracellular protein transport. We previously characterized two novel alleles to monitor Tnpo-SR localization (Beachum et al., 2023). Of these, a transgenic allele encoding a hemagglutinin-tagged Tnpo-SR (HA::Tnpo-SR) permitted specific and robust expression in the germline and faithfully reproduced endogenous Tnpo-SR intracellular localization in differentiated germ cells. We used this allele to carefully monitor Tnpo-SR localization in GSCs at different points in the cell cycle. As expected, we observed HA::Tnpo-SR around the nuclear membrane, inside the nucleus, and, to lesser extent, in the cytoplasm (Figure 5A-B), consistent with its purported role in nucleocytoplasmic transport. At mitosis, HA::Tnpo-SR was evenly dispersed between the nucleus and cytoplasm, demonstrating that it can freely traverse the semi-permeable nuclear lamina during mitosis (Figure 5C'). We also noted the existence of small puncta of HA::Tnpo-SR that were difficult to discern with standard confocal microscopy (Figure 5A'). Indeed, higher resolution imaging (with image deconvolution to improve the signal to noise ratio) confirmed that some HA::Tnpo-SR localized to vesicles, frequently near the nucleus and

of similar size as centrosomes (Figure 5B'). However, we did not observe HA::Tnpo-SR co-localized with α-Tubulin or the centrosome protein Asl, suggesting that it does not accumulate at centrosomes, fusomes, or the mitotic spindle. These data suggest that Tnpo-SR regulation of these organelles occurs indirectly.

Localization of Asp, but not other microtubule binding proteins, is regulated by Tnpo-SR.

Given its putative role as a nucleocytoplasmic transport protein, and the absence of co-localization at the fusome or centrosomes, we hypothesized that Tnpo-SR might function in the stability, transport, or translation of a protein essential for microtubule dynamics in germ cells. Previous studies identified Abnormal spindle (Asp), a microtubule binding protein that localizes to the poles of mitotic spindles and the minus ends of spindle microtubules, as a regulator of germ cell mitotic divisions (Riparbelli et al., 2004; Saunders et al., 1997). Originally described as a regulator of centrosome organization, loss of *asp* altered germ cell mitotic divisions (by inducing 'wavy' mitotic spindles), disrupted microtubule organization, and induced defects in fusome structure, similar to loss of *Tnpo-SR* (Beachum et al., 2023; Do Carmo Avides and Glover, 1999; Riparbelli et al., 2004; Saunders et al., 1997). Unfortunately, we were unable to source anti-Asp antibodies to visualize endogenous Asp. Instead, we confirmed Asp localization by driving a GFP-tagged Asp specifically in germ cells (Figures 6A, S3A) (Shao et al., 2010). Consistent with previous studies, Asp was enriched at the spindle poles and centrosomes during mitosis in GSCs and dividing cysts (Figure S3A). In interphase GSCs, however, Asp localized to the cytoplasm and was enriched at the fusome (Figure 6A,C). As germ cells differentiated, Asp remained localized to the cytoplasm until the 16-cell cyst stage, where it concentrated around the cortex of a single cyst cell (likely the presumptive oocyte) (Figure 6A,D). We then asked whether depletion of *Tnpo-SR* impacted Asp localization. In GSCs lacking *Tnpo-SR*, 40% of GSCs lost the cytoplasmic expression of Asp and instead concentrated it in the fusome (Figure 6B,C). Moreover, differentiated *Tnpo-SR*-depleted germ cells accumulated Asp in the nucleus, which was only rarely seen in controls (Figure 6B,D). These results suggest that *Tnpo-SR* is

necessary to move or stabilize Asp in the cytoplasm of GSCs and their differentiating daughters.

To determine whether the interaction between Tnpo-SR and Asp was specific, or a general property of effectors of spindle formation or disassembly, we examined localization of other regulators of microtubule dynamics. As with Asp, we used transgenic approaches to express a fluorescently-tagged version of each protein specifically in germ cells (Figure 7A-H and S3B-D). We selected three proteins associated with microtubule binding: Mini-Spindles (Msps), a plus-end microtubule binding protein that regulates microtubule organization (Brittle and Ohkura, 2005; Lu et al., 2023); Klp10A, a kinesin that induces microtubule depolymerization at plus ends (Chen et al., 2016; Persico et al., 2019); and an engineered kinesin-like protein that binds preferentially to microtubule minus ends (Khc::nod-lacZ; (Grieder et al., 2000)). In each case, microtubule binding proteins co-localized with α-Tubulin, and this localization was equivalent between control and *Tnpo-SR*-depleted GSCs (representative images from Khc::nod-lacZ and Msps are shown in Figure 7A-D). This suggests that Tnpo-SR specifically regulates Asp localization, rather than generally impacting localization of microtubule binding proteins.

Restoration of fusome morphogenesis is sufficient to rescue GSC loss in the absence of *Tnpo-SR*.

If the fusome promotes asymmetry between the GSC and the cystoblast during division, then failure to regenerate the fusome at each cell cycle should decrease GSC self-renewal, resulting in fewer numbers of GSCs in older flies. To test this idea, we asked whether restoration of fusome regeneration could rescue GSC loss in germaria that lack *Tnpo-SR*. To rescue fusome regeneration, we first over-expressed a fluorescently-tagged version of Hts in *Tnpo-SR*-depleted GSCs (Figure 7E-F). Notably, over-expression of Hts alone was not sufficient to change the area of the fusome in control GSCs. In the absence of *Tnpo-SR*, however, over-expression of Hts was sufficient to rescue fusome area in G_2/M (round fusomes) and G_1/S/G_2 (stretched

fusomes) (Figure 7I-J). Moreover, over-expression of Hts was also sufficient to rescue GSC number and the length of G_1 (Figure 7K-L, Table 1).

As an independent means to rescue fusome regeneration, we then over-expressed the polarity protein Baz (Figure 7G-H). Endogenous expression and localization of apical proteins (Baz, Scrib, or E-cadherin) was equivalent between *Tnpo-SR*-depleted and control cells (Figure S4) (Beachum et al., 2023). Since Baz is sufficient to promote microtubule focusing to the oocyte in differentiated cells (Cox et al., 2001; Huynh et al., 2001), we reasoned that over-expression of Baz might hyperpolarize GSCs, focusing microtubules to the apical border. Indeed, over-expression of a fluorescently tagged Baz alone or in *Tnpo-SR*-depleted GSCs significantly increased fusome area (Figure 7I-J). As with over-expression of Hts, over-expression of Baz in *Tnpo-SR*-depleted GSCs also rescued GSC number and the progression of these cells through G_1 (Figure 7K-L, Table 1).

Importantly, over-expression of other fusome-associated proteins was not sufficient to rescue fusome regeneration in the absence of *Tnpo-SR*. For example, fusome size in *Tnpo-SR*-depleted GSCs was not altered by over-expression of *sticky* (*sti*), a *Drosophila* ortholog of Citron Kinase that localizes to the GSC fusome and is essential for cytokinetic abscission (D'Avino and Capalbo, 2016; Price et al., 2023), or over-expression of the microtubule binding protein Klp10A (Figure 7I-L). Moreover, even though Asp localization was concentrated in the fusome in *Tnpo-SR*-depleted cells, its over-expression was not sufficient to restore fusome regeneration or GSC number (Table 1). This suggests that even though Tnpo-SR impacts Asp intracellular transport, this interaction is independent of the mechanism by which Tnpo-SR promotes fusome morphogenesis.

We also observed that over-expression of Khc::nod-lacZ was sufficient to rescue fusome size in *Tnpo-SR*-depleted cells only in cells in G_1/S/G_2, when the fusome is back-building from the cytokinetic furrow to the apical side of the GSC (Figure 7I-J). This effect also restored GSC number and the length of G_1 (Figure 7K-L). Since Khc::nod-lacZ binds microtubule minus ends, we propose that its over-expression helps extend, focus, and/or stabilize microtubules at the building fusome, promoting regeneration.

Surprisingly, although the over-expression of microtubule binding protein, Msps, did not rescue overall fusome integrity or G_1 progression in the absence of *Tnpo-SR*, we observed a significant increase in GSC number compared to loss of *Tnpo-SR* alone (Figure 7K). Previous studies showed that Msps is required to promote tubular ER formation through microtubule trafficking in later stage oocytes (Pokrywka et al., 2009). We propose that the over-expression of Msps may similarly increase the tubular ER of GSCs. Thus, although the fusome core size (visualized by Hts) was not altered, fusome/ER membrane area may have been increased sufficiently to restore fusome function and GSC maintenance in the absence of *Tnpo-SR*. Taken together, these results suggest that the fusome, which must be rebuilt in GSCs at each cell cycle, facilitates the intracellular protein trafficking that promotes GSC self-renewal.

Discussion

Stem cells that undergo ACD often have organelles that are partitioned asymmetrically, but whether organelle asymmetry promotes and maintains self-renewal is unknown. Here, we further characterized the roles of the β-importin, Tnpo-SR, in the regeneration and asymmetric distribution of the ER-like fusome in GSCs. We confirmed that a primary defect of *Tnpo-SR*-depleted cells is the loss of fusome area due to insufficient fusome regeneration at successive cell cycles. We found that consistent with roles described for other β-importins, Tnpo-SR maintains cystoskeletal organization through the suppression of microtubules during interphase and described a novel role for Tnpo-SR in nuclear lamina remodeling during mitosis. We also identified the microtubule binding protein, Asp, as a putative binding partner of Tnpo-SR. Although the over-expression of Asp itself was not sufficient to restore *Tnpo-SR* loss of function, restoration of fusome regeneration compensated for loss of *Tnpo-SR*, preserving GSC number. These data suggest that the primary function of the fusome is to establish and maintain an intracellular trafficking network to the apical pole of GSCs. Moreover, this intracellular trafficking is essential for maintaining GSCs in the niche over time. We propose that asymmetric distribution of the fusome is not only a hallmark of GSC biology, but also an integral part of maintaining the undifferentiated fate of GSCs.

Maintaining fusome integrity promotes GSC asymmetry.

In the interconnected germ cysts of the *Drosophila* ovary, the fusome acts to connect and coordinate germ cells via protein and organelle trafficking (Bolívar et al., 2001; Cox and Spradling, 2003; Deng and Lin, 1997; Grieder et al., 2000; Mahowald, 1971; Mahowald and Strassheim, 1970; Röper and Brown, 2004). As germline cysts mitotically divide, the fusome acts as an anchor for centrosomes, polarizing the mitotic spindles (Deng and Lin, 1997). In mutants lacking *hts*, mitotic divisions are randomized and cysts fragment (Deng and Lin, 1997). Further, the asymmetry of the fusome in differentiated cysts is required to establish oocyte identity. The fusome must coordinate and polarize microtubules to concentrate pro-oocyte factors asymmetrically (BicD, Egl, Orb) (Röper and Brown, 2004). Specialized structures like centromeres (Mahowald and Strassheim, 1970), centrosomes (Bolívar et al., 2001; Grieder et al., 2000), mitochondria (Cox and Spradling, 2003), and Golgi elements (Cox and Spradling, 2003) are then shuttled along the fusome and become concentrated in the oocyte. While the morphological changes of the fusome have been well described in asymmetric germ cells (GSC and oocyte), a direct role for the fusome in maintaining GSCs has not previously been described.

The molecular mechanisms directing fusome asymmetry in GSCs may be paralogous to the distribution of organelles across cell types (Barlan and Gelfand, 2017; Derivery et al., 2015; Jongsma et al., 2015; Ouellet and Barral, 2012). There are two evolutionary conserved principles that direct the separation of organelles. First, organelle inheritance must be spatially regulated. In yeast, this is regulated through interactions with microtubules (Ouellet and Barral, 2012; Weisman, 2006). Second, this process must be regulated in tune with the mitotic cell cycle (Ouellet and Barral, 2012; Weisman, 2003; Weisman, 2006). The latter of these rules seems to be much more complex among cell types because it relies on proper timing of organelle growth and cell cycle progression. In cells that undergo ACD, the process of organelle segregation is even more elaborate because the organelles themselves are asymmetrically segregated. For example, the distribution of ER in *Drosophila* neuroblasts relies on the

regulation of both polarity and microtubules, suggesting a positive feedback loop between organelle and microtubules dynamics (Smyth et al., 2015; Tikhomirova et al., 2022). We provide evidence suggesting that the ER-like fusome is asymmetrically segregated through a partnership with both microtubules and polarity factors. Coordinated with the mitotic cell cycle, the fusome relies on the stability of microtubules to asymmetrically segregate. In the absence of *Tnpo-SR*, interphase microtubule dynamics are disorganized and fusome integrity and asymmetry is diminished.

Interestingly, the over-expression of Msps in the absence of *Tnpo-SR* restored GSC maintenance independently of fusome area. In *Drosophila* oocytes, Msps works in tandem with minus-end microtubule motor, dynein, to create a positive feedback loop that enhances microtubule transport, creating a small but stochastic difference in microtubule polarity (Lu et al., 2023). Foundational studies on dynein and its transient presence in the fusome at mitosis suggest a role in polarizing the mitotic spindles of early germ cells (McGrail and Hays, 1997). The over-expression of Msps in the absence of *Tnpo-SR* could enhance microtubule polarity at levels sufficient to promote GSC asymmetry, but not enough to fully regenerate fusome area.

Importins are linked to several complex mitotic and meiotic regulatory events through their interaction with the RanGTPase cycle (Cesario and McKim, 2011; Kalab et al., 1999; Kalab et al., 2002; Lonhienne et al., 2009; Mühlhäusser and Kutay, 2007). The most extensive studies on the regulation of cytoskeletal organization by importins focused on Importin-α and Importin-β. For example, Importin-β maintains the mitotic spindle through associations with Ran in *C. elegans* embryos, and competitively binds the microtubule associated protein, NuMa, during interphase (Nachury et al., 2001; Wiese et al., 2001; Askjaer et al., 2002). Our analysis of *Tnpo-SR*-depleted GSCs suggests that Tnpo-SR shares some functional properties with Importin-β. While *Tnpo-SR* does not appear to influence mitotic spindle assembly or maintenance, it does play a significant role in the suppression of microtubules during interphase, similar to the interaction between Importin-B and NuMa.

To date, Tnpo-SR has only been directly implicated in the binding of phosphorylated serine/arginine (SR) proteins in *Drosophila* (Allemand et al., 2002; Lai et

al., 2001). Yet protein conformation studies in the human ortholog of Tnpo-SR, Tnpo3, identified over one hundred potential binding partners, ranging from transcription factors to microtubule and cell cycle regulators (Kimura et al., 2017). Although we cannot rule out the possibility that the effects we attribute to Tnpo-SR result from its interaction with a splicing factor (many of which are SR proteins), our data suggests Tnpo-SR may bind a variety of proteins that allow it to regulate multiple pathways.

We observed that localization of the minus-end microtubule binding protein, Asp, is altered in the absence of *Tnpo-SR*, and that localization of Asp is different in GSCs than in differentiated cells. This suggests a direct role for Tnpo-SR in maintaining Asp localization. However, we found no obvious evidence that Tnpo-SR and Asp co-localize, suggesting that this interaction may not be direct or stable. Importin partner proteins largely fall into two categories. “Cargoes” are proteins that are destined for transport, whereas “binding partners” can be transient or competitive interactions (Kuersten et al., 2001; Yang et al., 2023). Importin-β competitively binding microtubule associated protein, NuMa, during interphase is an example of an importin binding partner (Nachury et al., 2001; Wiese et al., 2001). Importin-β acts to sequester NuMa during interphase, suppressing ectopic microtubule assembly, but also allowing the nuclear accumulation of spindle assembly factors during interphase to ensure they are accessible near chromatin once mitosis begins. We propose that Asp is a binding partner of Tnpo-SR, most similar to the interaction between Importin-ß and NuMa. Alternatively, Tnpo-SR could impact localization of a factor necessary for Asp localization, or Tnpo-SR and Asp could interact with a common set of microtubule regulators. Additional studies will be necessary to elucidate relevant molecular mechanisms.

The changes in Asp localization depending on differentiation stage also suggests that importins like Tnpo-SR may regulate the developmental switches that occur during germ cell differentiation. Thus, while Tnpo-SR may serve to establish fusome asymmetry and thus maintain GSCs, it may likely play a different role in more differentiated germ cells, such as in establishment of oocyte identity or in the maintenance of fusome integrity necessary to keep differentiated cells interconnected. We posit that since Tnpo-SR promotes fusome morphogenesis, it may regulate GSC

maintenance and oocyte identity at least in part by some common molecular mechanisms, though unique regulation is also likely. Indeed, the difference in Asp localization suggests that not all mechanisms will be shared by GSCs and differentiated oocytes. Further studies investigating the cargo loads of Tnpo-SR based on differentiation stage will help distinguish between these possibilities.

Study Limitations

While this data supports that rescuing fusome regeneration is sufficient to promote GSC maintenance there are a few important limitations. We relied on over-expression of tagged proteins due to the low endogenous levels in GSCs, as this methodology allowed us to easily visualize proteins of interest. However, over-expression does not always reflect endogenous localization and could impact the localization or functionality of the protein. All studies were performed using fixed cell imaging. While we and others have demonstrated great reproducibility between fixed and live imaging of fusome dynamics, it remains formally possible that fixation of the samples alters intracellular localization of fusome-associated proteins.

Materials and Methods

Drosophila Strains and Husbandry

Flies were maintained at 22-25°C in standard medium (cornmeal/ molasses/yeast/agar) (NutriFly MF; Genesee Scientific). Fly genotypes are listed in Table 2. Female progeny were collected within 24 h of eclosion and maintained on wet yeast at 25°C. For RNAi experiments, germline knockdown of *Tnpo-SR* was facilitated by expressing the *pValium22*-based transgene *UAS-Tnpo-SR*^{RNAi} using the germline-specific *nos-GAL4::VP16-nos.UTR* (referred to throughout as *nos-Gal4*) (Beachum et al., 2023; Doren et al., 1998). Females carrying the driver alone were used as controls.

Tnpo-SR null GSCs (Figure S4) were generated by inducing genetic mosaics using *Flippase (FLP)/FLP recognition target (FRT)* mitotic recombination, as previously described (Beachum et al., 2023).

Immunofluorescence and Microscopy

Ovaries were prepared for immunofluorescence microscopy as described (Hinnant et al., 2017; Williams and Ables, 2023). Ovaries were dissected and teased apart in room temperature Grace's medium without additives (Caisson Labs) and fixed in 5.3% formaldehyde in Grace's medium for 10 min at room temperature. They were then washed extensively in phosphate-buffered saline (PBS, pH 7.4; Fisher) with 0.1% Triton X-100, permeabilized in PBS with 0.5% Triton X-100 for 30 minutes and blocked for 3 hours in blocking solution [5% normal goat serum (MP Biomedicals), and 0.1% Triton X-100 in PBS] at room temperature. Primary antibodies (listed in Table 2) were diluted in blocking solution and used overnight at 4°C. Secondary antibodies were followed by a 2 hour (or overnight) incubation at room temperature with AlexaFluor 488-, 568- or 633-conjugated goat species-specific antibodies (Life Technologies; 1:200).

All ovary samples were stained with 0.5 µg/ml 40 -6-diamidino-2- phenylindole (DAPI; Sigma) in 0.1% Triton X-100 in PBS, and mounted in 90% glycerol mixed with 20% n-propyl gallate (Sigma). Confocal z-stacks (1 or 0.5 µm optical sections) were collected with the Zeiss LSM700 laser scanning microscope or Zeiss LSM800 laser scanning microscope with Airyscan detector both using Zen Black software. Airyscan images were subject to deconvolution protocols performed by the Zen program. Images were analyzed using Zeiss ZEN software or FIJI and minimally and equally enhanced via histogram using ZEN and Adobe Photoshop Creative Suite.

Statistical Analysis

GSCs were identified based on the juxtaposition of their fusomes to the junction of adjacent cap cells. GSC loss was measured as the average number of GSCs per germaria, and results were subjected to a Student's two-tailed T-test comparing *(Figures 1,3,4)* driver controls versus *driver>UAS-RNAi* or (Figure 7) *driver>UAS-RNAi* versus *driver>UAS-RNAi,UASp* rescue model. Each experimental group was evaluated using Microsoft Excel and Prism (Graphpad).

Fusome measurements were taken from the center-most z-stack of each GSC where the main bulk of the fusome was most highly localized. The average pixel area of the fusome was collected using the FIJI area tool measuring the pixel area of the identified fusome using α-Hts, α-alpha-Spec, or α-GFP (Scrib::GFP, Rtnl1::GFP). Measurements were transferred to Microsoft Excel and Student's two-tailed T-tests were performed comparing driver controls versus *driver>UAS-RNAi* versus *driver>UAS-RNAi,UASp* rescue model.

Mitotic spindle measurements were taken using the line tool in FIJI using a max z-stack projection of the mitotic GSC being analyzed (from the bottom of the cell to the top). Length measurements were collected from one centrosome to the other (identified by centrosome marker Asl). Width measurements were taken from the center of the mitotic spindle at its widest point. Measurements were transferred to Microsoft Excel and Student's two-tailed T-tests were performed comparing driver controls versus *driver>UAS-RNAi* versus *driver>UAS-RNAi,UASp* rescue model.

Interphase microtubules were identified based on the presence of alpha-tubulin emanating from centrosomes (identified by centrosome marker Asl). A Fishers Exact test analysis was performed using Prism (Graphpad) comparing driver controls versus *driver>UAS-RNAi* versus *driver>UAS-RNAi,UASp* rescue model.

Intensity of LaminB accumulation at the DNA during mitosis measurements were taken using the line tool in FIJI. Each mitotic GSC was visualized in a z-stack max projection and a line was drawn surrounding the DNA (using DAPI to visualize). The intensity of LaminB was measured at that line and measurements were transferred to Microsoft Excel and Students two-tailed T-tests were performed comparing driver controls versus *driver>UAS-RNAi.*

Acknowledgements

Many thanks to the ECU Department of Biology Microscopy Core Facilities and the ECU School of Dental Medicine for microscopy support, and to members of the Ables and Anllo laboratories and our anonymous reviewers for helpful discussion and critical reading of this manuscript. *Drosophila* lines were obtained from the Bloomington

Drosophila Stock Center (NIH P40OD018537) or Kyoto *Drosophila* stock center or kind gifts from V. Gefland, A. Spradling, D. Drummond-Barbosa, T. Harris, and B. Riggs. Antibodies were a kind gift from N. Rusan or obtained from the Developmental Studies Hybridoma Bank (DSHB), created by the NICHD of the NIH and maintained at the University of Iowa, Department of Biology.

Competing Interests

No competing interests declared.

Funding

This work was supported by National Institutes of Health R15-GM117502 (E. T. A.). A.M.P. was supported by the East Carolina University Department of Biology, Harriot College of Arts and Sciences, and Graduate School. A.E.W. was supported by the ECU Office of Undergraduate Research.

Data and Resource Availability

Data and resource availability: All relevant data and resource can be found within the article and its supplementary information.

References

Ables, E. T. and Drummond-Barbosa, D. (2013). Cyclin E controls *Drosophila* female germline stem cell maintenance independently of its role in proliferation by modulating responsiveness to niche signals. *Development* **140**, 530–540.

Allemand, E., Dokudovskaya, S., Bordonné, R. and Tazi, J. (2002). A conserved Drosophila transportin-serine/arginine-rich (SR) protein permits nuclear import of Drosophila SR protein splicing factors and their antagonist repressor splicing factor 1. *Mol. Biol. Cell* **13**, 2436–2447.

Askjaer, P., Galy, V., Hannak, E. and Mattaj, I. W. (2002). Ran GTPase Cycle and Importins α and β Are Essential for Spindle Formation and Nuclear Envelope Assembly in Living *Caenorhabditis elegans* Embryos. *Mol. Biol. Cell* **13**, 4355–4370.

Barlan, K. and Gelfand, V. I. (2017). Microtubule-Based Transport and the Distribution, Tethering, and Organization of Organelles. *Cold Spring Harb. Perspect. Biol.* **9**, a025817.

626 **Beachum, A. N., Hinnant, T. D., Williams, A. E., Powell, A. M. and Ables, E. T.** (2023). β-
627 importin Tnpo-SR promotes germline stem cell maintenance and oocyte differentiation in
628 female Drosophila. *Dev. Biol.* **494**, 1–12.

629 **Beaudet, D., Akhshi, T., Phillipp, J., Law, C. and Piekny, A.** (2017). Active Ran regulates
630 anillin function during cytokinesis. *Mol. Biol. Cell* **28**, 3517–3531.

631 **Beaudet, D., Pham, N., Skaik, N. and Piekny, A.** (2020). Importin binding mediates the
632 intramolecular regulation of anillin during cytokinesis. *Mol. Biol. Cell* **31**, 1124–1139.

633 **Bogard, N., Lan, L., Xu, J. and Cohen, R. S.** (2007). Rab11 maintains connections between
634 germline stem cells and niche cells in the *Drosophila* ovary. *Development* **134**, 3413–
635 3418.

636 **Bolívar, J., Huynh, ean-R., López-Schier, H., González, C., Johnston, D. S. and González-**
637 **Reyes, A.** (2001). Centrosome migration into the *Drosophila* oocyte is independent of
638 *BicD* and *egl* , and of the organisation of the microtubule cytoskeleton. *Development*
639 **128**, 1889–1897.

640 **Brittle, A. L. and Ohkura, H.** (2005). Mini spindles, the XMAP215 homologue, suppresses
641 pausing of interphase microtubules in Drosophila. *EMBO J.* **24**, 1387–1396.

642 **Cesario, J. and McKim, K. S.** (2011). RanGTP is required for meiotic spindle organization and
643 the initiation of embryonic development in *Drosophila*. *J. Cell Sci.* **124**, 3797–3810.

644 **Chaigne, A. and Brunet, T.** (2022). Incomplete abscission and cytoplasmic bridges in the
645 evolution of eukaryotic multicellularity. *Curr. Biol.* **32**, R385–R397.

646 **Chen, C. and Yamashita, Y. M.** (2021). Centrosome-centric view of asymmetric stem cell
647 division. *Open Biol.* **11**, 200314.

648 **Chen, A., Akhshi, T. K., Lavoie, B. D. and Wilde, A.** (2015). Importin β2 Mediates the Spatio-
649 temporal Regulation of Anillin through a Noncanonical Nuclear Localization Signal. *J.*
650 *Biol. Chem.* **290**, 13500–13509.

651 **Chen, C., Inaba, M., Venkei, Z. G. and Yamashita, Y. M.** (2016). Klp10A, a stem cell
652 centrosome-enriched kinesin, balances asymmetries in Drosophila male germline stem
653 cell division. *eLife* **5**, e20977.

654 **Cox, R. T. and Spradling, A. C.** (2003). A Balbiani body and the fusome mediate mitochondrial
655 inheritance during *Drosophila* oogenesis. *Development* **130**, 1579–1590.

656 **Cox, D. N., Lu, B., Sun, T.-Q., Williams, L. T. and Jan, Y. N.** (2001). Drosophila par-1 is
657 required for oocyte differentiation and microtubule organization. *Curr. Biol.* **11**, 75–87.

658 **Das, D., Fletcher, R. B. and Ngai, J.** (2020). Cellular mechanisms of epithelial stem cell self-
659 renewal and differentiation during homeostasis and repair. *WIREs Dev. Biol.* **9**, e361.

660 **Dattoli, A. A., Carty, B. L., Kochendoerfer, A. M., Morgan, C., Walshe, A. E. and Dunleavy,**
661 **E. M.** (2020). Asymmetric assembly of centromeres epigenetically regulates stem cell
662 fate. *J. Cell Biol.* **219**, e201910084.

D'Avino, P. P. and Capalbo, L. (2016). Regulation of midbody formation and function by mitotic kinases. *Semin. Cell Dev. Biol.* **53**, 57–63.

de Cuevas, M. and Spradling, A. C. (1998). Morphogenesis of the Drosophila fusome and its implications for oocyte specification. *Dev. Camb. Engl.* **125**, 2781–2789.

de Cuevas, M., Lee, J. K. and Spradling, A. C. (1996). alpha-spectrin is required for germline cell division and differentiation in the Drosophila ovary. *Dev. Camb. Engl.* **122**, 3959–3968.

de Cuevas, M., Lilly, M. A. and Spradling, A. C. (1997). Germline cyst formation in Drosophila. *Annu. Rev. Genet.* **31**, 405–428.

de Morree, A. and Rando, T. A. (2023). Regulation of adult stem cell quiescence and its functions in the maintenance of tissue integrity. *Nat. Rev. Mol. Cell Biol.* **24**, 334–354.

Deng, W. and Lin, H. (1997). Spectrosomes and fusomes anchor mitotic spindles during asymmetric germ cell divisions and facilitate the formation of a polarized microtubule array for oocyte specification in Drosophila. *Dev. Biol.* **189**, 79–94.

Derivery, E., Seum, C., Daeden, A., Loubéry, S., Holtzer, L., Jülicher, F. and Gonzalez-Gaitan, M. (2015). Polarized endosome dynamics by spindle asymmetry during asymmetric cell division. *Nature* **528**, 280–285.

Diegmiller, R., Imran Alsous, J., Li, D., Yamashita, Y. M. and Shvartsman, S. Y. (2023). Fusome topology and inheritance during insect gametogenesis. *PLOS Comput. Biol.* **19**, e1010875.

Do Carmo Avides, M. and Glover, D. M. (1999). Abnormal Spindle Protein, Asp, and the Integrity of Mitotic Centrosomal Microtubule Organizing Centers. *Science* **283**, 1733–1735.

Doren, M. V., Williamson, A. L. and Lehmann, R. (1998). Regulation of zygotic gene expression in Drosophila primordial germ cells. *Curr. Biol.* **8**, 243–246.

Duan, T., Cupp, R. and Geyer, P. K. (2021). Drosophila female germline stem cells undergo mitosis without nuclear breakdown. *Curr. Biol. CB* **31**, 1450-1462.e3.

Fichelson, P., Moch, C., Ivanovitch, K., Martin, C., Sidor, C. M., Lepesant, J.-A., Bellaiche, Y. and Huynh, J.-R. (2009). Live-imaging of single stem cells within their niche reveals that a U3snoRNP component segregates asymmetrically and is required for self-renewal in Drosophila. *Nat. Cell Biol.* **11**, 685–693.

Grieder, N. C., de Cuevas, M. and Spradling, A. C. (2000). The fusome organizes the microtubule network during oocyte differentiation in Drosophila. *Dev. Camb. Engl.* **127**, 4253–4264.

Hinnant, T. D., Alvarez, A. A. and Ables, E. T. (2017). Temporal remodeling of the cell cycle accompanies differentiation in the Drosophila germline. *Dev. Biol.* **429**, 118–131.

Hinnant, T. D., Merkle, J. A. and Ables, E. T. (2020). Coordinating Proliferation, Polarity, and Cell Fate in the Drosophila Female Germline. *Front. Cell Dev. Biol.* **8**, 19.

Huynh, J.-R. (2006). Fusome as a Cell-Cell Communication Channel of Drosophila Ovarian Cyst. In *Cell-Cell Channels*, pp. 217–235. New York, NY: Springer New York.

Huynh, J.-R., Petronczki, M., Knoblich, J. A. and Johnston, D. S. (2001). Bazooka and PAR-6 are required with PAR-1 for the maintenance of oocyte fate in Drosophila. *Curr. Biol.* **11**, 901–906.

Jongsma, M. L. M., Berlin, I. and Neefjes, J. (2015). On the move: organelle dynamics during mitosis. *Trends Cell Biol.* **25**, 112–124.

Kalab, P., Pu, R. T. and Dasso, M. (1999). The ran GTPase regulates mitotic spindle assembly. *Curr. Biol. CB* **9**, 481–484.

Kalab, P., Weis, K. and Heald, R. (2002). Visualization of a Ran-GTP gradient in interphase and mitotic Xenopus egg extracts. *Science* **295**, 2452–2456.

Kimura, M., Morinaka, Y., Imai, K., Kose, S., Horton, P. and Imamoto, N. (2017). Extensive cargo identification reveals distinct biological roles of the 12 importin pathways. *eLife* **6**, e21184.

Knoblich, J. A. (2008). Mechanisms of Asymmetric Stem Cell Division. *Cell* **132**, 583–597.

Koch, E. A. and King, R. C. (1966). The origin and early differentiation of the egg chamber of *Drosophila melanogaster*. *J. Morphol.* **119**, 283–303.

Kochendoerfer, A. M., Modafferi, F. and Dunleavy, E. M. (2021). Centromere function in asymmetric cell division in *Drosophila* female and male germline stem cells. *Open Biol.* **11**, 210107.

Kuersten, S., Ohno, M. and Mattaj, I. W. (2001). Nucleocytoplasmic transport: Ran, beta and beyond. *Trends Cell Biol.* **11**, 497–503.

Lai, M. C., Lin, R. I. and Tarn, W. Y. (2001). Transportin-SR2 mediates nuclear import of phosphorylated SR proteins. *Proc. Natl. Acad. Sci. U. S. A.* **98**, 10154–10159.

Li, L. and Xie, T. (2005). STEM CELL NICHE: Structure and Function. *Annu. Rev. Cell Dev. Biol.* **21**, 605–631.

Li, Z. P., Moreau, H., Petit, J. D., Moraes, T. S., Smokvarska, M., Pérez-Sancho, J., Petrel, M., Decoeur, F., Brocard, L., Chambaud, C., et al. (2024). Plant plasmodesmata bridges form through ER-dependent incomplete cytokinesis. *Science* **386**, 538–545.

Lighthouse, D. V., Buszczak, M. and Spradling, A. C. (2008). New components of the Drosophila fusome suggest it plays novel roles in signaling and transport. *Dev. Biol.* **317**, 59–71.

Lin, H., Yue, L. and Spradling, A. C. (1994). The *Drosophila* fusome, a germline-specific organelle, contains membrane skeletal proteins and functions in cyst formation. *Development* **120**, 947–956.

Lonhienne, T. G., Forwood, J. K., Marfori, M., Robin, G., Kobe, B. and Carroll, B. J. (2009). Importin-beta is a GDP-to-GTP exchange factor of Ran: implications for the mechanism of nuclear import. *J. Biol. Chem.* **284**, 22549–22558.

Lu, X., Shi, Y., Lu, Q., Ma, Y., Luo, J., Wang, Q., Ji, J., Jiang, Q. and Zhang, C. (2010). Requirement for Lamin B Receptor and Its Regulation by Importin β and Phosphorylation in Nuclear Envelope Assembly during Mitotic Exit. *J. Biol. Chem.* **285**, 33281–33293.

Lu, W., Lakonishok, M. and Gelfand, V. I. (2023). *Drosophila* oocyte specification is maintained by the dynamic duo of microtubule polymerase Mini spindles/XMAP215 and dynein.

Mahowald, A. P. (1971). Polar granules of *Drosophila* . III. The continuity of polar granules during the life cycle of *Drosophila*. *J. Exp. Zool.* **176**, 329–343.

Mahowald, A. P. and Strassheim, J. M. (1970). INTERCELLULAR MIGRATION OF CENTRIOLES IN THE GERMARIUM OF *DROSOPHILA MELANOGASTER*. *J. Cell Biol.* **45**, 306–320.

Mathieu, J., Cauvin, C., Moch, C., Radford, S. J., Sampaio, P., Perdigoto, C. N., Schweisguth, F., Bardin, A. J., Sunkel, C. E., McKim, K., et al. (2013). Aurora B and Cyclin B Have Opposite Effects on the Timing of Cytokinesis Abscission in Drosophila Germ Cells and in Vertebrate Somatic Cells. *Dev. Cell* **26**, 250–265.

McGrail, M. and Hays, T. S. (1997). The microtubule motor cytoplasmic dynein is required for spindle orientation during germline cell divisions and oocyte differentiation in *Drosophila*. *Development* **124**, 2409–2419.

Mühlhäusser, P. and Kutay, U. (2007). An in vitro nuclear disassembly system reveals a role for the RanGTPase system and microtubule-dependent steps in nuclear envelope breakdown. *J. Cell Biol.* **178**, 595–610.

Nachury, M. V., Maresca, T. J., Salmon, W. C., Waterman-Storer, C. M., Heald, R. and Weis, K. (2001). Importin beta is a mitotic target of the small GTPase Ran in spindle assembly. *Cell* **104**, 95–106.

Ong, S., Foote, C. and Tan, C. (2010). Mutations of DMYPT cause over constriction of contractile rings and ring canals during Drosophila germline cyst formation. *Dev. Biol.* **346**, 161–169.

Ouellet, J. and Barral, Y. (2012). Organelle segregation during mitosis: Lessons from asymmetrically dividing cells. *J. Cell Biol.* **196**, 305–313.

Persico, V., Callaini, G. and Riparbelli, M. G. (2019). The Microtubule-Depolymerizing Kinesin-13 Klp10A Is Enriched in the Transition Zone of the Ciliary Structures of Drosophila melanogaster. *Front. Cell Dev. Biol.* **7**, 173.

Pokrywka, N. J., Payne-Tobin, A., Raley-Susman, K. M. and Swartzman, S. (2009). Microtubules, the ER and Exu: New associations revealed by analysis of mini spindles mutations. *Mech. Dev.* **126**, 289–300.

Price, K. L., Tharakan, D. M. and Cooley, L. (2023). Evolutionarily conserved midbody remodeling precedes ring canal formation during gametogenesis. *Dev. Cell* **58**, 474-488.e5.

Qi, H., Rath, U., Wang, D., Xu, Y.-Z., Ding, Y., Zhang, W., Blacketer, M. J., Paddy, M. R., Girton, J., Johansen, J., et al. (2004). Megator, an Essential Coiled-Coil Protein that Localizes to the Putative Spindle Matrix during Mitosis in *Drosophila*. *Mol. Biol. Cell* **15**, 4854–4865.

Rath, U., Wang, D., Ding, Y., Xu, Y., Qi, H., Blacketer, M. J., Girton, J., Johansen, J. and Johansen, K. M. (2004). Chromator, a novel and essential chromodomain protein interacts directly with the putative spindle matrix protein skeletor. *J. Cell. Biochem.* **93**, 1033–1047.

Riparbelli, M. G., Massarelli, C., Robbins, L. G. and Callaini, G. (2004). The abnormal spindle protein is required for germ cell mitosis and oocyte differentiation during Drosophila oogenesis. *Exp. Cell Res.* **298**, 96–106.

Röper, K. (2007). Rtnl1 is enriched in a specialized germline ER that associates with ribonucleoprotein granule components. *J. Cell Sci.* **120**, 1081–1092.

Röper, K. and Brown, N. H. (2004). A Spectraplakin Is Enriched on the Fusome and Organizes Microtubules during Oocyte Specification in Drosophila. *Curr. Biol.* **14**, 99–110.

Saunders, R. D. C., Avides, M. D. C., Howard, T., Gonzalez, C. and Glover, D. M. (1997). The *Drosophila* Gene *abnormal spindle* Encodes a Novel Microtubule-associated Protein That Associates with the Polar Regions of the Mitotic Spindle. *J. Cell Biol.* **137**, 881–890.

Shao, W., Wu, J., Chen, J., Lee, D. M., Tishkina, A. and Harris, T. J. C. (2010). A Modifier Screen for Bazooka/PAR-3 Interacting Genes in the Drosophila Embryo Epithelium. *PLoS ONE* **5**, e9938.

Smyth, J. T., Schoborg, T. A., Bergman, Z. J., Riggs, B. and Rusan, N. M. (2015). Proper symmetric and asymmetric endoplasmic reticulum partitioning requires astral microtubules. *Open Biol.* **5**, 150067.

Snapp, E. L., Iida, T., Frescas, D., Lippincott-Schwartz, J. and Lilly, M. A. (2004). The Fusome Mediates Intercellular Endoplasmic Reticulum Connectivity in *Drosophila* Ovarian Cysts. *Mol. Biol. Cell* **15**, 4512–4521.

Spradling, A. C. (2024). The Ancient Origin and Function of Germline Cysts. In *Syncytia: Origin, Structure, and Functions* (ed. Kloc, M.) and Uosef, A.), pp. 3–21. Cham: Springer International Publishing.

Sunchu, B. and Cabernard, C. (2020). Principles and mechanisms of asymmetric cell division. *Development* **147**, dev167650.

Tikhomirova, M. S., Kadosh, A., Saukko-Paavola, A. J., Shemesh, T. and Klemm, R. W. (2022). A role for endoplasmic reticulum dynamics in the cellular distribution of microtubules. *Proc. Natl. Acad. Sci.* **119**, e2104309119.

Venkei, Z. G. and Yamashita, Y. M. (2015). The centrosome orientation checkpoint is germline stem cell specific and operates prior to the spindle assembly checkpoint in *Drosophila* testis. *Development* **142**, 62–69.

Villa-Fombuena, G., Lobo-Pecellín, M., Marín-Menguiano, M., Rojas-Ríos, P. and González-Reyes, A. (2021). Live imaging of the Drosophila ovarian niche shows spectrosome and centrosome dynamics during asymmetric germline stem cell division. *Dev. Camb. Engl.* **148**, dev199716.

Weisman, L. S. (2003). Yeast Vacuole Inheritance and Dynamics. *Annu. Rev. Genet.* **37**, 435–460.

Weisman, L. S. (2006). Organelles on the move: insights from yeast vacuole inheritance. *Nat. Rev. Mol. Cell Biol.* **7**, 243–252.

Weitzman, M. D. and Wang, J. Y. J. (2013). Cell Cycle: DNA Damage Checkpoints. In *Encyclopedia of Biological Chemistry*, pp. 410–416. Elsevier.

Wiese, C., Wilde, A., Moore, M. S., Adam, S. A., Merdes, A. and Zheng, Y. (2001). Role of Importin-β in Coupling Ran to Downstream Targets in Microtubule Assembly. *Science* **291**, 653–656.

Williams, A. E. and Ables, E. T. (2023). Visualizing Fusome Morphology via Tubulin Immunofluorescence in Drosophila Ovarian Germ Cells. In *Drosophila Oogenesis* (ed. Giedt, M. S.) and Tootle, T. L.), pp. 135–150. New York, NY: Springer US.

Yamashita, Y. M., Mahowald, A. P., Perlin, J. R. and Fuller, M. T. (2007). Asymmetric Inheritance of Mother Versus Daughter Centrosome in Stem Cell Division. *Science* **315**, 518–521.

Yang, Y., Guo, L., Chen, L., Gong, B., Jia, D. and Sun, Q. (2023). Nuclear transport proteins: structure, function and disease relevance. *Signal Transduct. Target. Ther.* **8**, 425.

Yao, C., Rath, U., Maiato, H., Sharp, D., Girton, J., Johansen, K. M. and Johansen, J. (2012). A nuclear-derived proteinaceous matrix embeds the microtubule spindle apparatus during mitosis. *Mol. Biol. Cell* **23**, 3532–3541.

Yao, C., Wang, C., Li, Y., Zavortink, M., Archambault, V., Girton, J., Johansen, K. M. and Johansen, J. (2018). Evidence for a role of spindle matrix formation in cell cycle progression by antibody perturbation. *PLOS ONE* **13**, e0208022.

Zielke, N., Korzelius, J., van Straaten, M., Bender, K., Schuhknecht, G. F. P., Dutta, D., Xiang, J. and Edgar, B. A. (2014). Fly-FUCCI: A versatile tool for studying cell proliferation in complex tissues. *Cell Rep.* **7**, 588–598.

Figures

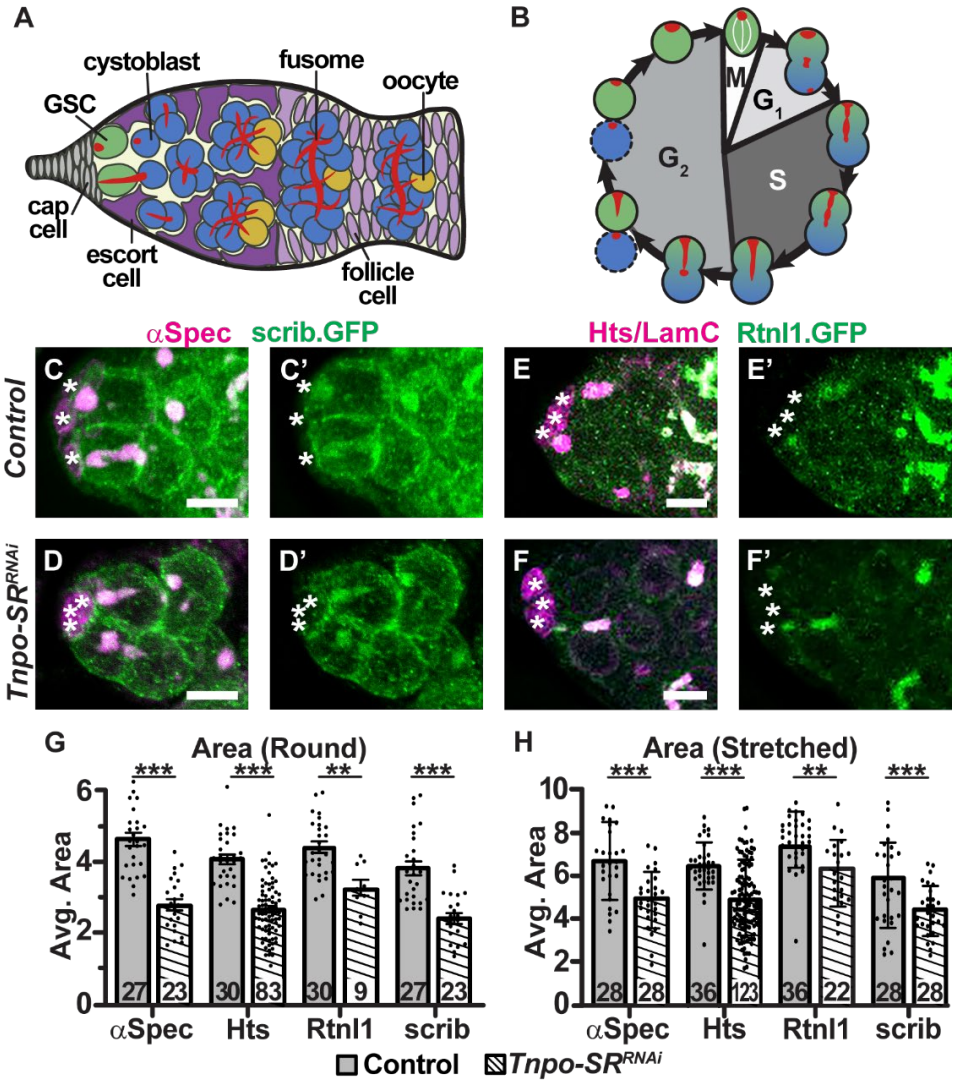

Figure 1: *Tnpo-SR* promotes GSC fusome regeneration. (A) Schematic of *Drosophila* germarium. Somatic cap cells (grey) are juxtaposed to GSCs (green). Asymmetric division of a GSC yields a cystoblast (blue) which divides four times through incomplete cytokinesis to produce a 16-cell interconnected cyst. One cyst cell becomes the oocyte (yellow). The fusome (red) interconnects germ cells. (B) Fusome morphogenesis parallels progression through the cell cycle. (C-F) Max projections of germaria from *Scrib::GFP* (green, C-D) or *Rtnl1::GFP* (green, E-F) control females (C, E) or combined with *Tnpo-SR*^{RNAi} (D, F), immunostained for fusome core proteins α-Spectrin (C-D, magenta) and Hts (E-F, magenta; with LamC to visualize cap cells). Asterisks (*) denote cap cells. Scale bars = 5μm. (G-H) Quantification of fusome area in round (G) and stretched (H) fusome morphologies. Numbers in bars represent number of GSCs analyzed. Error bars represent s.e.m. (***)p<0.00001, (**)p<0.0001; Student's two-tailed T-test.

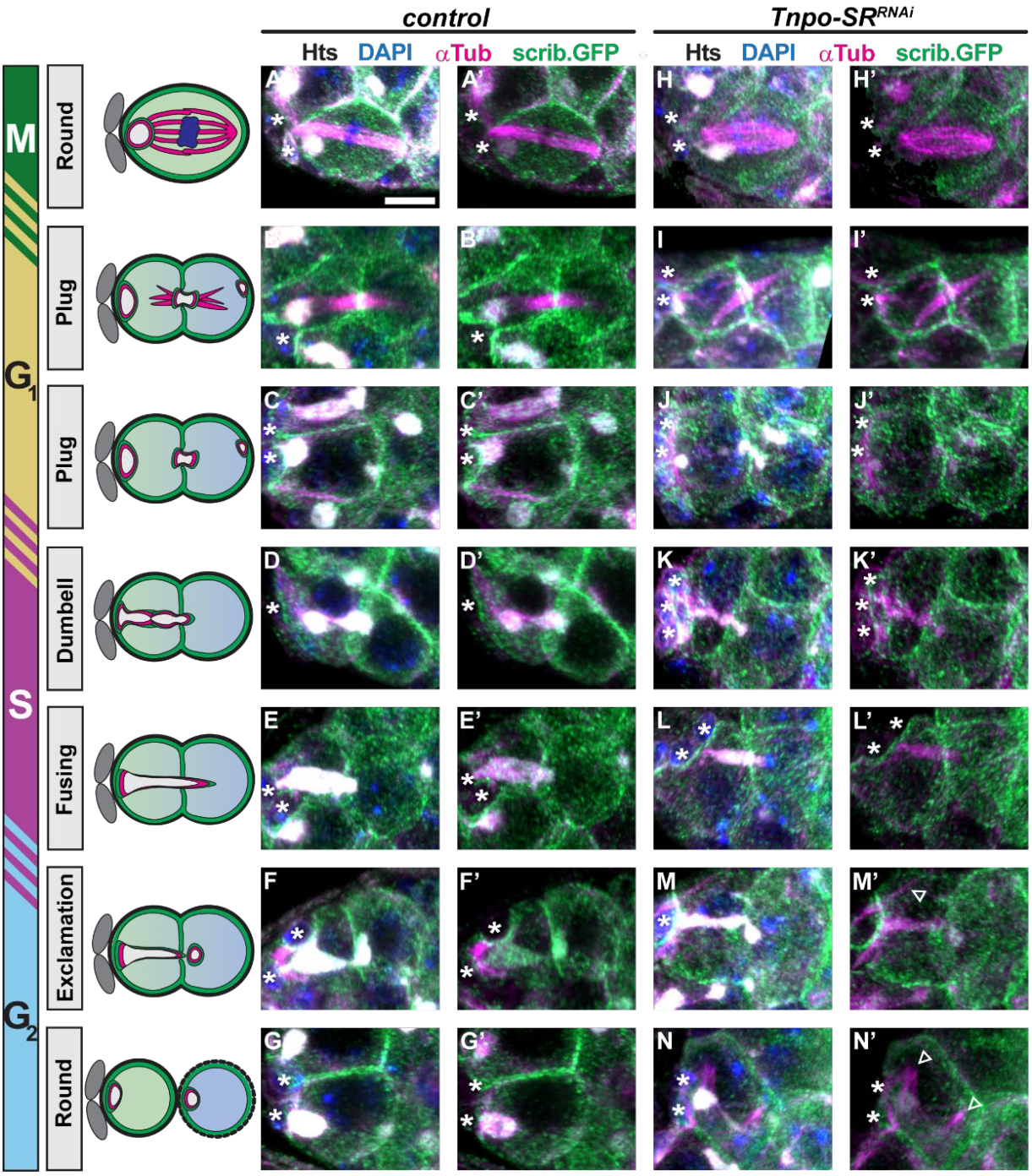

Figure 2: *Tnpo-SR* maintains fusome asymmetry. (A-G) Control and (I-N) *Tnpo-SR*^{RNAi} GSCs immunostained for the fusome (Hts, white), microtubules (α-Tub, magenta), polarity and cell membrane marker Scrib (Scrib::GFP, green), and DNA (DAPI, blue). Graphics represent the wild-type fusome morphological changes and the subsequent localization of Hts, Scrib and αTub as GSCs go through the cell cycle. Asterisks denote cap cells. Scale bar = 5μm. Arrowheads denote microtubule defects (M', N').

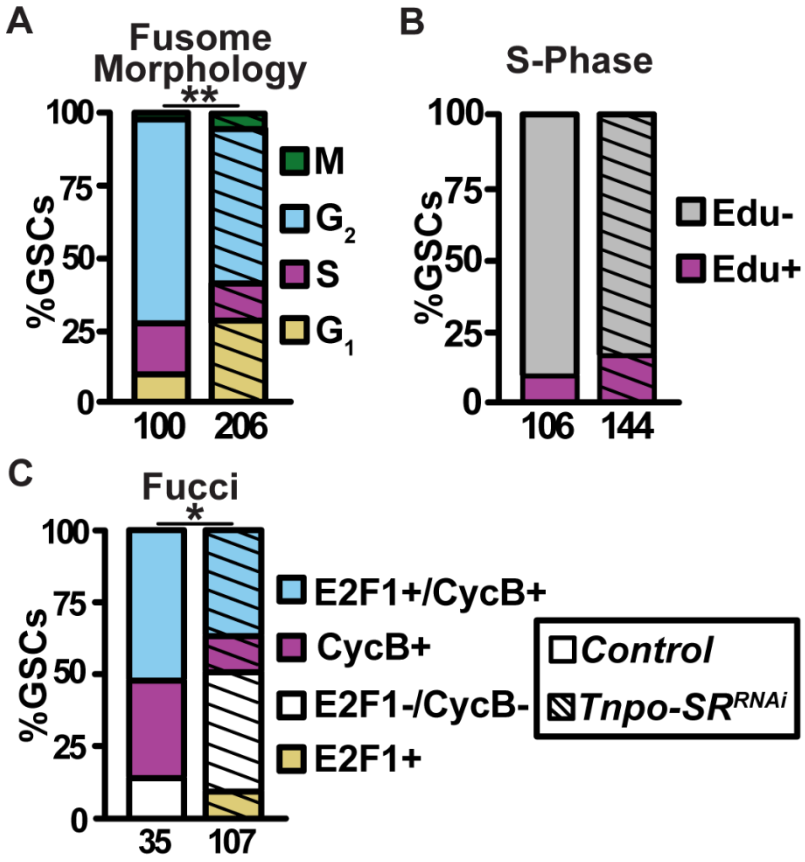

Figure 3: Loss of *Tnpo-SR* delays exit from G_1. Quantification of cell cycle progression via fusome morphology (A), incorporation of EdU in a one-hour pulse (B), or Fly-FUCCI fluorescent labeling (C) in control (solid) or *Tnpo-SR*^{RNAi} (striped) GSCs. G_1 (yellow and white), S (purple), G_2 (blue), M (green). Mitotic GSCs were identified by chromosome morphology (labeled with DAPI). (B) Percentage GSCs that are EDU positive (purple) or negative (grey). Numbers below bars indicate number of GSCs analyzed. Fisher's Exact test was used to compare the number of GSCs in G_1 (plug morphology, A; E2F1+, C) or the number of EdU+ GSCs (B) to the total number of GSCs. (**)$p<0.001$, (*)$p<0.01$.

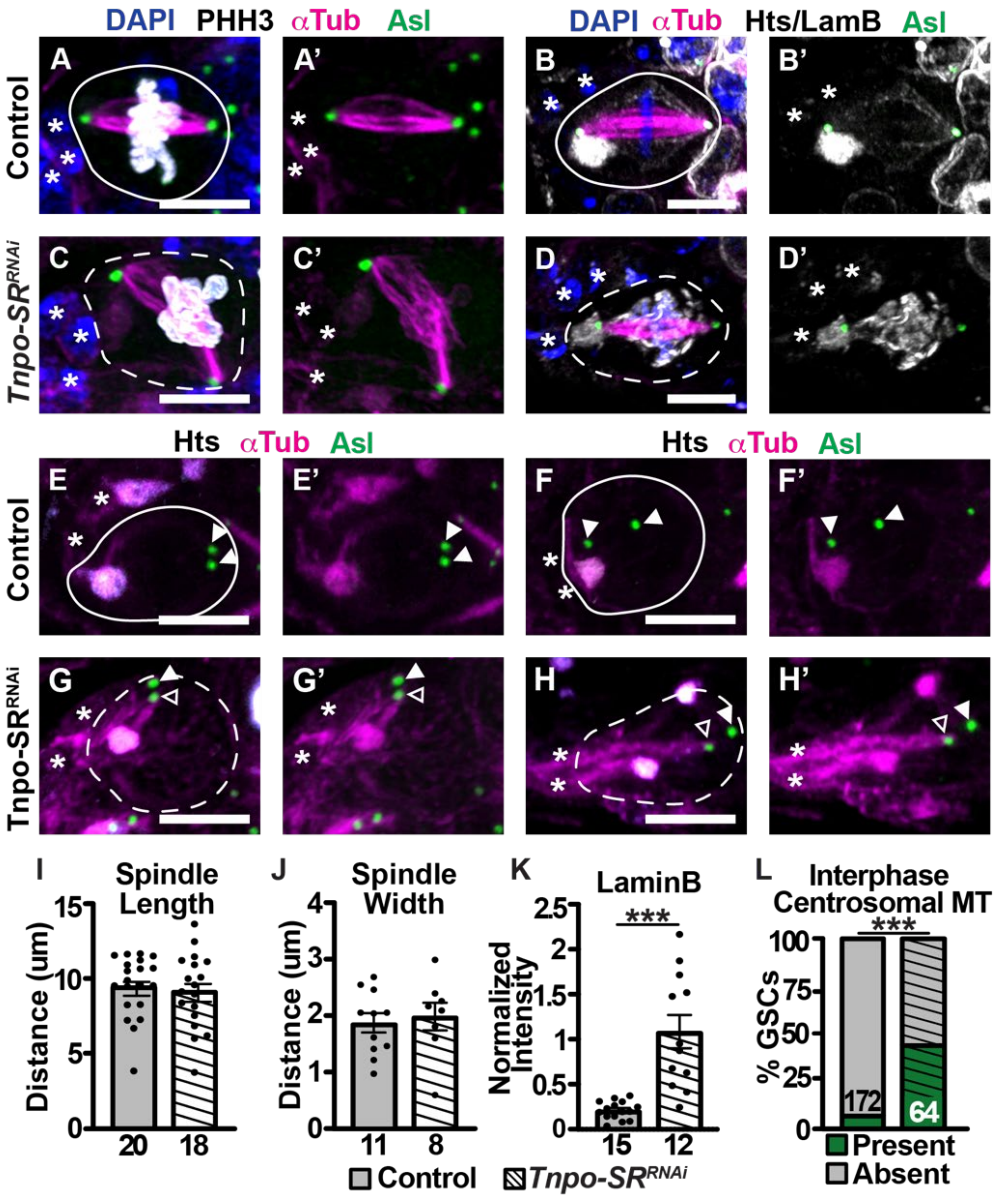

Figure 4: *Tnpo-SR* regulates nuclear lamina remodeling at mitosis and suppresses microtubule growth during interphase. (A-H) Control (A-B,E-F), and *Tnpo-SR*^{RNAi} (C-D,G-H) germaria immunostained for a mitotic marker (PHH3, white) (A,C), the fusome (Hts, white) (B,D-H), microtubules (α-Tubulin, magenta), centrosomes (Asl, green), and DNA (DAPI) (A-D). GSCs outlined with white lines (solid, control) (dashed, Tnpo-SR^{RNAi}). Asterisks denote cap cells. Scale bars = 5μm. (I-L) Quantification of GSC mitotic spindle length (I) and width (J), LaminB fluorescence intensity (K), and interphase GSCs with microtubules emanating from centrosomes (L) in control (solid) or *Tnpo-SR*^{RNAi} (striped) germaria. Numbers in/under bars represent number of GSCs analyzed. Error Bars represent s.e.m. (***)p<0.00001, (**)p<0.0001; Student's two-tailed T-test (I-K) or Fishers Exact test (L).

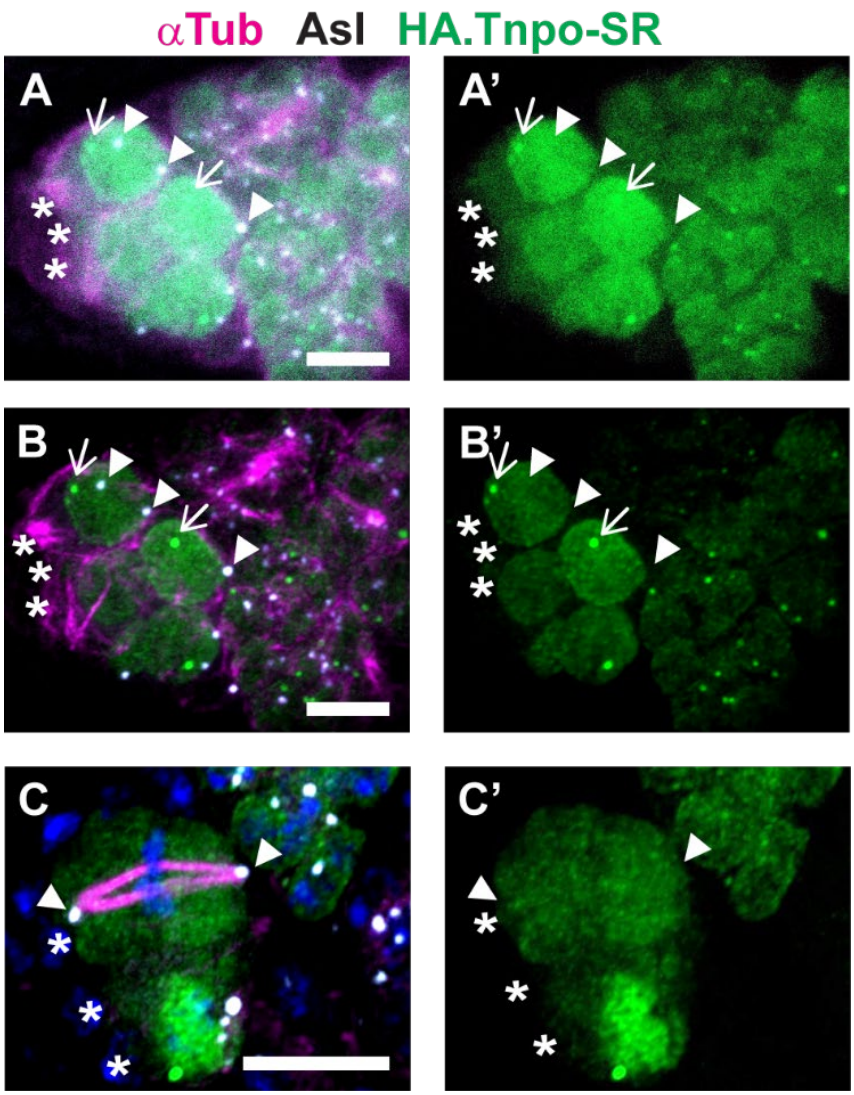

Figure 5: Tnpo-SR does not aggregate in fusomes or at centrosomes. Maximum intensity projections of interphase (A-B) or mitotic (C) *UASz-HA::Tnpo-SR* GSCs immunostained for Tnpo-SR (HA, green), microtubules (α-Tubulin, magenta), centrosomes (Asl, white), and DNA (DAPI, blue). A-B are the same germarium imaged with (B) and without (A) Airyscan high resolution imaging with deconvolution. Asterisks denote cap cells. Arrowheads denote centrosomes (Asl). Arrows denote HA-enriched foci. Scale bar = 5μm.

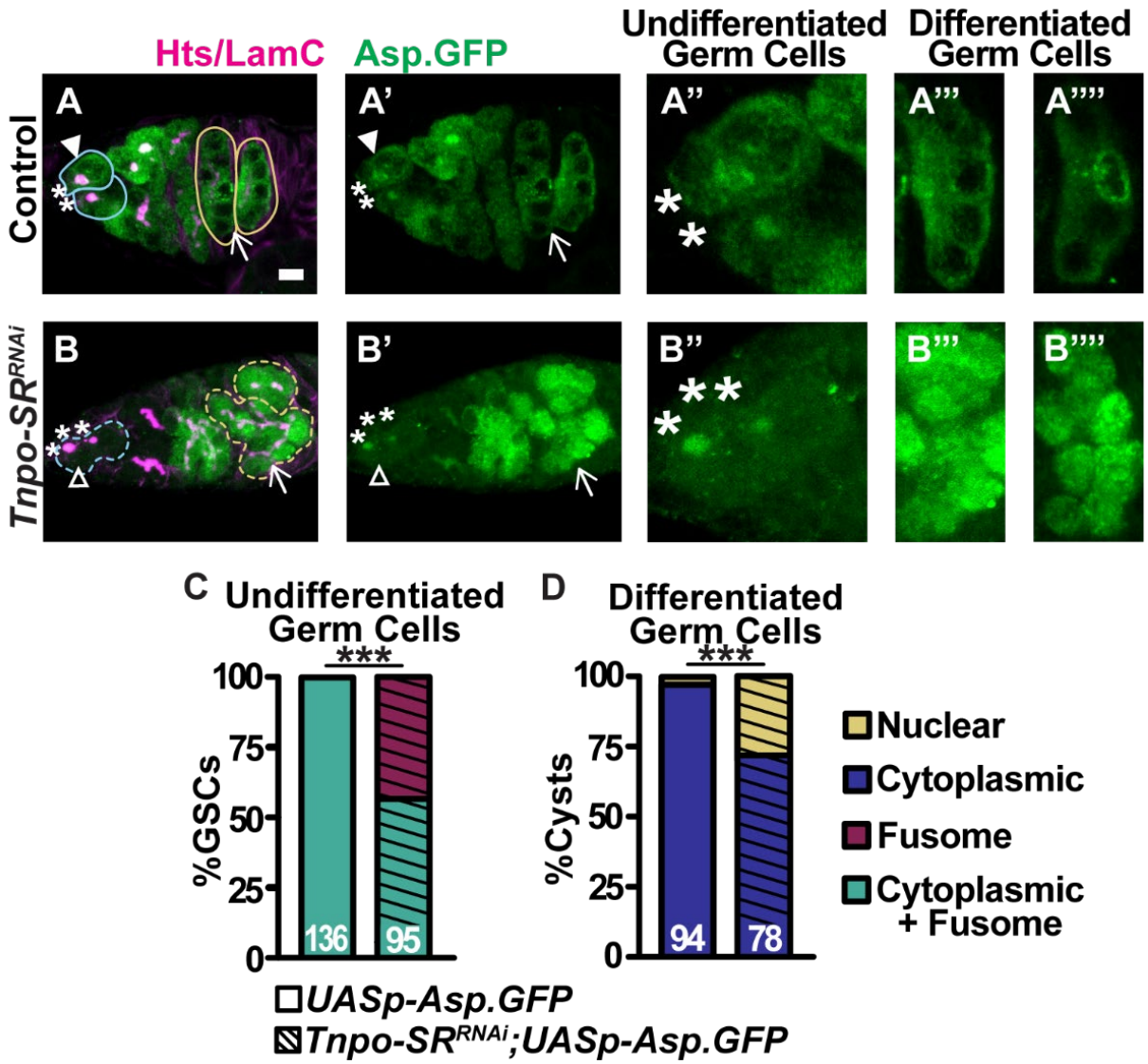

Figure 6: Asp intracellular localization is regulated by *Tnpo-SR*. (A-B) *UASp-Asp::GFP* (A) and *Tnpo-SR^{RNAi};UASp-Asp::GFP* (B) germaria immunostained for the fusome (Hts, magenta), cap cells (LamC, magenta), and Asp (green). Asterisks denote cap cells, blue lines outline GSCs, yellow lines outline differentiated germ cells, arrow heads denote Asp localization in undifferentiated germ cells, arrows denote Asp localization in differentiated germ cells. Scale bar = 5μm. (C-D) Quantification of Asp localization in control (solid) and *Tnpo-SR^{RNAi};UASp-Asp::GFP* (striped) GSCs (C) or differentiated germ cells (D). Numbers in bars represent numbers of GSCs (C) or cysts (D). (***)p<0.00001, Fishers Exact test.

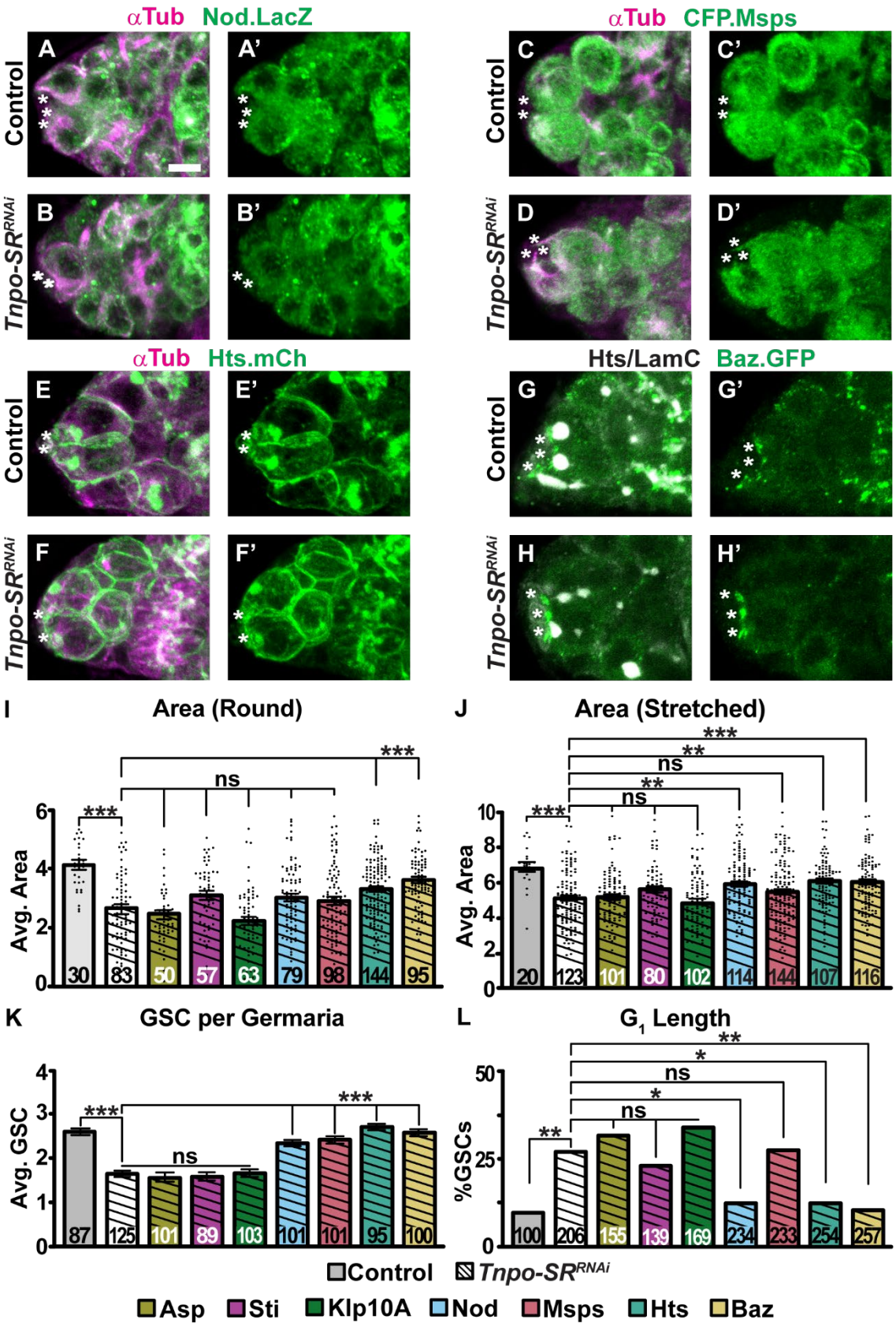

Figure 7: Restoration of fusome regeneration rescues GSC self-renewal and G_1 length in *Tnpo-SR*-depleted GSCs. Representative germaria from control (A,C,E,G) or *Tnpo-SR*^{RNAi} (B,D,F,H) females carrying *UASp-Khc::nod::LacZ* (A-B), *UASp-CFP::Msps* (C-D), *UASp-Hts::mCherry* (E-F), or *UASp-Baz::GFP* (G-H), immunostained for α-Tubulin (αTub, magenta, A-F) and β-galactosidase (A-B), GFP (C-D, G-H), or mCherry (E-F) to visualize the tagged proteins. Asterisks denote cap cells. Scale bars = 5μm. (I-J) Quantification of fusome area in round (I) and stretched (J) fusome morphologies. (K) Quantification of the number of GSCs per germarium, as a readout of GSC self-renewal. (L) Quantification of cell cycle progression via fusome morphology. Numbers in bars represent number of GSCs (I-J,L) or germaria (K). Error bars represent s.e.m. Controls (solid bars) were compared to *Tnpo-SR*^{RNAi} alone (white striped bars), while *Tnpo-SR*^{RNAi} alone was compared to *Tnpo-SR*^{RNAi} combined with over-expression of the indicated gene of interest (stripes with colors) using Student's two-tailed T-test (I-K) [(***)p<0.00001, (**)p<0.0001] or Fishers Exact test (L) [(**)p<0.001, (*)p<0.01].

Table 1: Summary of rescue phenotypes in *Tnpo-SR*-depleted GSCs. Original data (Figure 7) is summarized, indicating the raw data for average (Avg.) GSC per germaria, pixelated area of round and stretched fusomes, and the percentage of GSCs in G_1 when the cell cycle was quantified based on fusome morphology. P-value statistics were determine by comparisons made using Student's two-tailed T-test For Avg. GSC and fusome measurements [(***)p<0.00001, (**)p<0.0001] or Fishers Exact test (%G_1) [(**)p<0.001, (*)p<0.01] for fusome morphology data.

	Round Fusome		Stretched Fusome		Avg. GSC		Cell Cycle Phase	
	Area	**P-value**	**Area**	**P-value**	**GSC#**	**P-value**	**%G_1**	**P-value**
Control* vs. *Tnpo-SR^{RNAi}								
Tnpo-SR^{RNAi}	2.7 (***)	9.5E-9	4.9 (***)	4.0E-5	1.6 (***)	3.5E-18	28% (**)	0.0019
Tnpo-SR^{RNAi}* vs. *UASp-O/E ; Tnpo-SR^{RNAi}								
UASp-Asp	2.52	0.342	5.02	0.779	1.537	0.396	32%	0.539
UASp-Sti	3.18	0.018	5.5	0.029	1.56	0.507	25%	0.629
UASp-Klp10A	2.24	0.012	4.6	0.140	1.62	0.877	35%	0.361
UASp-Nod	3.07	0.039	5.8 (**)	0.0001	2.3 (***)	1.2E-9	13% (*)	0.014
UASp-Msps	2.98	0.132	5.3	0.088	2.4 (***)	4.4E-11	29%	0.999
UASp-Hts	3.3 (***)	8.7E-5	5.9 (**)	0.0001	2.7 (***)	9.8E-20	13% (*)	0.014
UASp-Baz	3.7 (***)	1.1E-8	5.9 (***)	3.0E-5	2.6 (***)	8.2E-16	11% (**)	0.004

1036 **Table 2. Reagents.** List of fly lines and antibodies used in this study.

***Drosophila* Strains**			
Shorthand	***Genotype***	***Description***	***Available From***
nosGal4::VP16	*w[1118]; P{w[+mC]=GAL4::VP16-nanos.UTR}CG6325[MVD1]*	germline-specific Gal4	BDSC #4937
UASp-LacZ	*P{w[+mC]=UASp-lacZ}1, w[*]*	expresses ß-gal under UASp control	BDSC #98113
Tnpo-SR^{RNAi}	*y[1] sc[*] v[1] sev[21]; P{y[+t7.7] v[+t1.8]=TRiP.HMC04414}attP40*	Expresses dsRNA for RNAi of Tnpo-SR under UAS control	BDSC #56974
UASz-HA:Tnpo-SR	*P{UASz-HA-Tnpo-SR}2.1 attP40*	Overexpression of Tnpo-SR with an N Terminus HA tag	Beachum et al. 2023
Scrib::GFP	*w[*]; P{w[+mC]=PTT-GA}scrib[CA07683]*	Expresses GFP-tagged scribble protein in the native pattern	Gift from A. Spradling BDSC #94708
Rtln::GFP	*Rtnl1-GFP[G00199]*	Expresses GFP-tagged reticulon protein in the native pattern	Gift from B. Riggs
FUCCI	*w1118; P{UASp-GFPE2f.1-230}26P{UASp-mRFP1.CycB.1-266}81;MKRS/TM6B, Tb+*	Expresses E2f and CycB degrons fused to fluorescent proteins.	BDSC #55100
UASp-mCh.Sti	*w[*]; P{w[+mC]=UASp-ChFP.sti}20/CyO*	Overexpression of Sticky (Sti) with a N Terminus mCherry tag	BDSC #81648
UASp-Asp.GFP	*w[*]; P{y[+t7.7] w[+mC]=UASp-asp.GFP}attP2*	Overexpression of Abnormal Spindle (Asp) with a C Terminus GFP tag	BDSC #65859
UASp-Klp10A.GFP	*yw; Sp/CyO; UASp-Klp10A-GFP-SspB(w+) (M2, III)/(TM3)*	Overexpression of Klp10A with a C Terminus GFP tag	Gift from V. Gefland

UASp-Msps.GFP	*w; UASp-CFP-Msps-CDS 96E (III)/TM6B*	Overexpression of Mini Spindles (Msps) with a C Terminus GFP tag	Gift from V. Gefland
UASp-Nod.LacZ	*w[*]; P{w[+mC]=UASp-Khc::nod::lacZ}3/TM3, Sb[1]*	Overexpression of Non Distributive Disjunction (Nod) with a C Terminus ß-gal tag	BDSC #29723
UASp-Hts.mCh	*w[*]; P{w[+mC]=UASp-hts.mCherry}attP2*	Overexpression of Hts with a C Terminus mCherry tag	Gift from T. Harris BDSC #66171
UASp-Baz::GFP	*w[*];* *P{y[+t7.7] w[+mC]=UASp-baz.C.GFP}attP2*	Overexpression of Bazooka (Baz) with a C Terminus GFP tag	BDSC #65845
Tnpo-SR^{KG04870}	*y[d2] w[1118] P{ry[+t7.2]=eyFLP.N}2 P{ry[+t7.2]=GMR-lacZ.C(38.1)}TPN1; P{y[+mDint2]w[BR.E.BR]=SUPor P}TrnSR[KG04870] P{ry[+t7.2]=neoFRT}40A / CyO, y[+]*	Tnpo-SR^{KG} mutant allele	KDSC #111581
HsFlp;Frt40A	*hsFLP;(FRT40A.ubiGFP/cyo)*	Flp;FRT Clonal driver	Gift from D. Drummond-Barbosa

Antibodies

Abbreviation	***Animal and Clonality***	***Available From***
GFP	Chicken, polyclonal	Abcam #AB_13970
RFP	Rabbit, polyclonal	Clontech #632496
β-Gal	Chicken, polyclonal	Abcam #AB_9361
PHH3	Rabbit, polyclonal	Millipore #06-570
Hts (1B1)	Mouse, monoclonal	DSHB #AB_528070

α-Spectrin (3A9)	Mouse, monoclonal	DSHB #AB_528473
Lamin C (LC28.26)	Mouse, monoclonal	DSHB #AB_528339
Lamin B (ADL84.12)	Mouse, monoclonal	DSHB #AB_528338
α-Tub 555, 647	Mouse, monoclonal	Millipore #05829-555
Hemagglutinin (HA)	Rat, monoclonal	Roche Tech. #11867423001
Asterless (Asl)	Guinea Pig, monoclonal	Gift from N. Rusan
Pericentrin-Like-Protein (Plp)	Rabbit, monoclonal	Gift from N. Rusan
EdU Click-iT Kit		Invitrogen #C10638

1037